

Experimental prediction of deformation mechanism after continuous dynamic recrystallization in superplastic P/M7475

T. HIRATA*

Department of Metallurgy and Materials Science, Graduate School of Engineering, Osaka Prefecture University, Gakuen-cho, Sakai, Osaka 599-8531, Japan
E-mail: hirata@tri.pref.osaka.jp

T. MUKAI

Osaka Municipal Technical Research Institute, 1-6-50 Morinomiya, Joto-ku, Osaka 536-8553, Japan

N. SAITO

National Institute of Advanced Industrial Science and Technology, Moriyama-ku, Nagoya 463-8687, Japan

S. TANABE, M. KOHZU, K. HIGASHI

Department of Metallurgy and Materials Science, Osaka Prefecture University, Gakuen-cho, Sakai, Osaka 599-8531, Japan

The deformation mechanism in high-strain-rate superplastic P/M7475 before and after continuous dynamic recrystallization (CDRX) was investigated. The recrystallization process in P/M7475 differed from that in conventional superplastic material, I/M7475. In I/M7475, the fine-grained microstructure was obtained by static recrystallization before deformation. On the other hand, the substructure in P/M7475 evolved into fine grains during deformation by CDRX. The percentage of high-angle and random boundaries was low at an initial stage of deformation. However, it increased with strain in P/M7475. The microstructural change in P/M7475 influenced a deformation mechanism and affected grain boundary sliding (GBS). The ratio of contribution of GBS to total elongation was low at an early stage of deformation in P/M7475. However, it increased with deformation progressed. It is suggested that the deformation behavior in P/M7475 changed from dislocation creep to superplasticity as the dominant deformation mechanism changed to GBS. The activation energy for superplastic flow in P/M7475 was close to that for lattice self-diffusion in pure aluminum. It is therefore concluded that the dominant deformation mechanism after CDRX in P/M7475 is GBS accommodated by dislocation movement controlled by lattice self-diffusion, similar to that in I/M7475. © 2003 Kluwer Academic Publishers

1. Introduction

It is well known that 7475 aluminum alloy processed by ingot metallurgy (I/M7475) exhibits extensive superplasticity [1–9]. In addition, it has been reported that 7475 alloy containing Zr processed by powder metallurgy (P/M7475) exhibited high-strain-rate superplasticity [8–13]. Recently, a body of knowledge has been developed about the superplasticity of aluminum alloys attained at relatively high strain rates (over 10^{-2} s^{-1}) [8–16]. The strain rates over 10^{-2} s^{-1} is comparable to the commercial hot working rates, so that the superplastic forming is suitable for commercial applications. In aluminum alloys, high-strain-rate superplasticity is generally associated with continuous dynamic recrystallization (CDRX).

It is well known that the superplastic strain rate increases with refining grain size in the aluminum alloys [17]. It has already been reported that superplastic aluminum alloys such as Al-Cu-Zr (Supral) [18–20] and Al-Mg-Zr [10, 15, 16] developed fine grains by CDRX and exhibited high-strain-rate superplasticity associated with their very small grain sizes. P/M7475 also developed fine grains by CDRX during hot deformation. Much of the work on the superplastic P/M7475 alloy has focused on the high rate at which it forms [8–14].

The microstructural changes involved in P/M7475 superplasticity may be considered to influence a deformation mechanism. In superplastic deformation, the

*Current address: Technology Research Institute of Osaka Prefecture, 2-7-1 Ayumino, Izumi, Osaka 594-1157, Japan.

dominant deformation mechanism is recognized to be grain boundary sliding (GBS) [21, 22]. It has been reported that GBS was influenced by grain boundary character (GBC) [23, 24]. The microstructural change in P/M7475 is expected to affect GBS. It has been reported a lot about the deformation mechanism in I/M7475 [1–6]. However, the deformation mechanism in P/M7475 is not fully understood yet. The relationship between the deformation mechanism and grain boundary microstructure received some attention in our former paper [9]. This line of inquiry was completed in the present paper. In addition, the deformation mechanism in P/M7475 before and after CDRX was investigated in comparison to I/M7475 and found to be related with grain boundary character distribution (GBCD). In order to clarify the accommodation process in P/M7475, the activation energy for superplastic flow in P/M7475 was evaluated.

2. Experimental procedure

The materials in the present study were P/M7475 (Al-5.4Zn-2.1Mg-1.5Cu-0.2Cr-0.7Zr) and I/M7475 (Al-5.8Zn-2.6Mg-1.5Cu-0.2Cr). I/M7475 was used for

comparison with the results of P/M7475. Initial microstructures in P/M7475 and I/M7475 are shown in Fig. 1. The initial grain sizes in P/M7475 and I/M7475 were $2.5\ \mu\text{m}$ and $14\ \mu\text{m}$ in average with, respectively. These materials were received in a sheet form with a thickness of 1.5 mm. The sheets were machined into flat tensile samples parallel to the rolling direction with a gauge length of 16 mm and a gauge width of 8 mm. Constant strain rate tests and jump strain rate tests were carried out on an Instron type testing machine controlled by computer. The m value was estimated by jump strain rate test in which the strain rate difference was -30% between the base and the jump, and was calculated by the difference of flow stress. The decreased strain rate maintained for a short time. The GBCD was examined by Orientation Imaging Microscopy (OIM). The OIM is a completely automated system for orientation measurements based on automated indexing of electron backscatter Kikuchi diffraction patterns [25]. In the present study, GBC was divided into three categories, low-angle boundaries ($\theta < 15^\circ$), high-angle boundaries, which satisfied the criteria for nearness to coincident site lattice (CSL) relations of up to $\Sigma 29$ boundaries ($\theta \geq 15^\circ$), and random boundaries ($\theta \geq 15^\circ$).

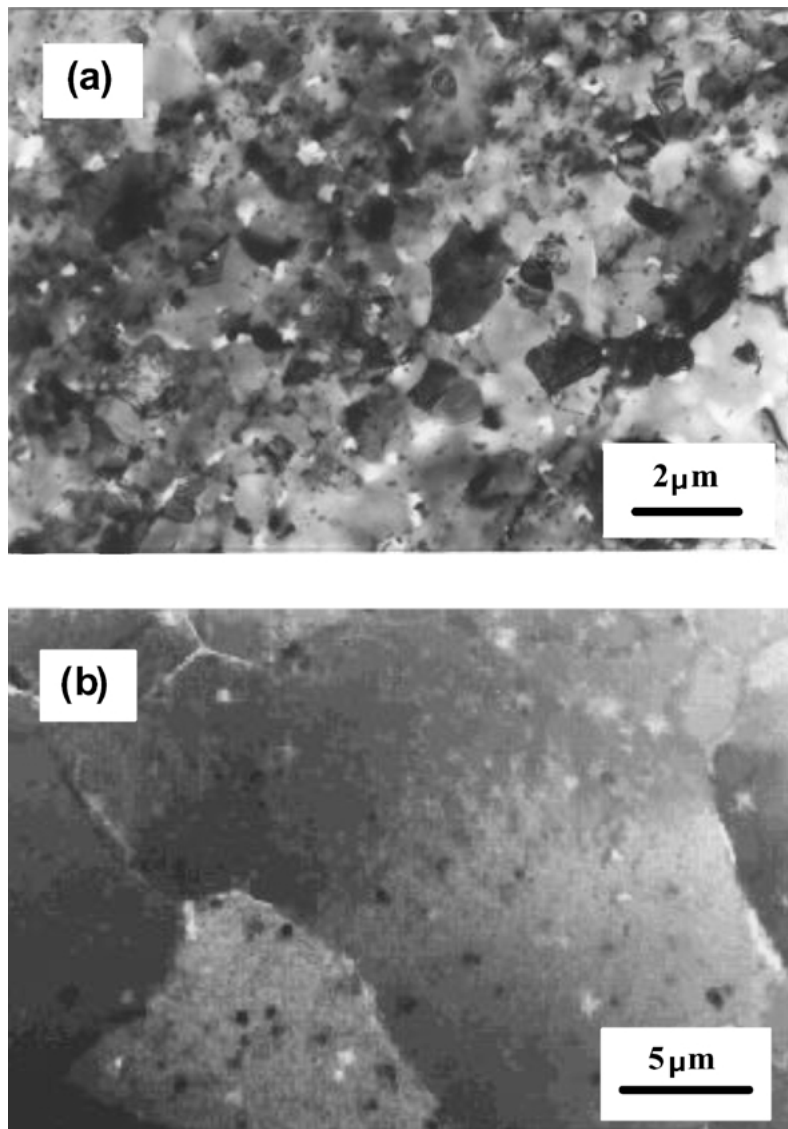


Figure 1 The initial microstructures in (a) P/M7475 and (b) I/M7475.

The contribution of GBS to the macroscopic elongation was also estimated quantitatively. Before deformation, the specimen surface was electrolytically polished and the marker lines were scribed for sliding measurement on the surface parallel to the tensile axis. The tensile tests were stopped at each strain and quenched in water quickly. The surface appearance of the deformed specimen was inspected by a scanning electron microscopy (SEM) in order to measure the amount of GBS from the offsets of the marker lines. The contribution of GBS to total elongation, r_{GBS} was calculated by $\varepsilon_{\text{GBS}}/\varepsilon_{\text{TOT}}$, where ε_{GBS} was the elongation by GBS and ε_{TOT} was the total elongation. The r_{GBS} at many position was calculated, then the average value was estimated.

3. Results

3.1. Characterization of superplastic flow in conventional superplastic material

3.1.1. Deformation mechanism in I/M7475

High temperature deformation mechanisms can be represented by a constitutive equation. When a threshold stress, σ_{th} , is taken into consideration, the mechanical properties for superplastic deformation may be described by an equation for power-law creep of the form [26, 27]:

$$\dot{\varepsilon} = \frac{ADGb}{kT} \left(\frac{\sigma - \sigma_{\text{th}}}{G} \right)^n \left(\frac{b}{d} \right)^p. \quad (1)$$

where $\dot{\varepsilon}$ is the steady-state strain rate, D is the appropriate diffusion coefficient ($D = D_0 \exp(-Q/RT)$, where D_0 is the frequency factor), Q is the activation energy for the diffusion process, R is the gas constant, T is the absolute temperature, G is the shear modulus, b is the Burgers vector, k is Boltzmann's constant, d is the grain size, σ is the applied stress, p is the grain size exponent, n is the stress exponent ($= 1/m$: strain rate sensitivity exponent), and A is the material constant.

In I/M7475, it has been reported that $n = 2$, $p = 2$, $Q = Q_{\text{L}}$ for Equation 1 at superplastic deformation, where Q_{L} is the activation energy for lattice self-diffusion. The I/M7475 data of the present study and the other reported data [1–6] are normalized for superplastic behavior. The relationship between $(\dot{\varepsilon}/D_{\text{L}})(kT/Gb)(d/b)^2$ and $(\sigma - \sigma_{\text{th}})/G$ for I/M7475 is illustrated in Fig. 2, where D_{L} is the lattice diffusion coefficient for pure aluminum [28]. In superplastic region, from an extrapolation to zero strain rate of a line in a double-linear scale relation $\sigma = \dot{\varepsilon}^{1/n}$ (where $n = 2$ in the present study), the threshold stress can be estimated [26]. It is obviously noted that the superplastic behavior in I/M7475 is represented by a single straight line with a slope of 2 in the normalized plot compensated by the lattice diffusion coefficient for pure aluminum. In this way, the figure shows that the present data in the superplastic region for I/M7475 is in good agreement with the previous investigation. Therefore, the constitutive equation for I/M7475 exhibiting superplastic behavior may be given by

$$\dot{\varepsilon} = 3.73 \times 10^5 \frac{D_{\text{L}}Gb}{kT} \left(\frac{\sigma - \sigma_{\text{th}}}{G} \right)^2 \left(\frac{b}{d} \right)^2. \quad (2)$$

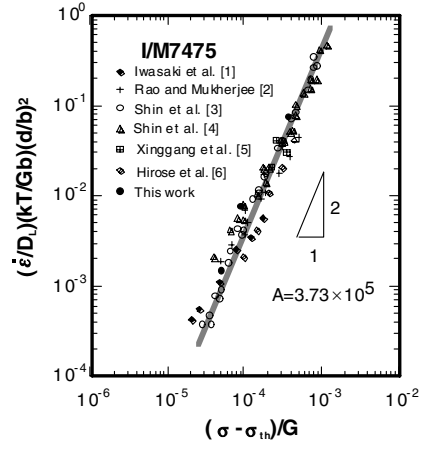


Figure 2 Relationship between $(\dot{\varepsilon}/D_{\text{L}})(kT/Gb)(d/b)^2$ and $(\sigma - \sigma_{\text{th}})/G$ for I/M7475.

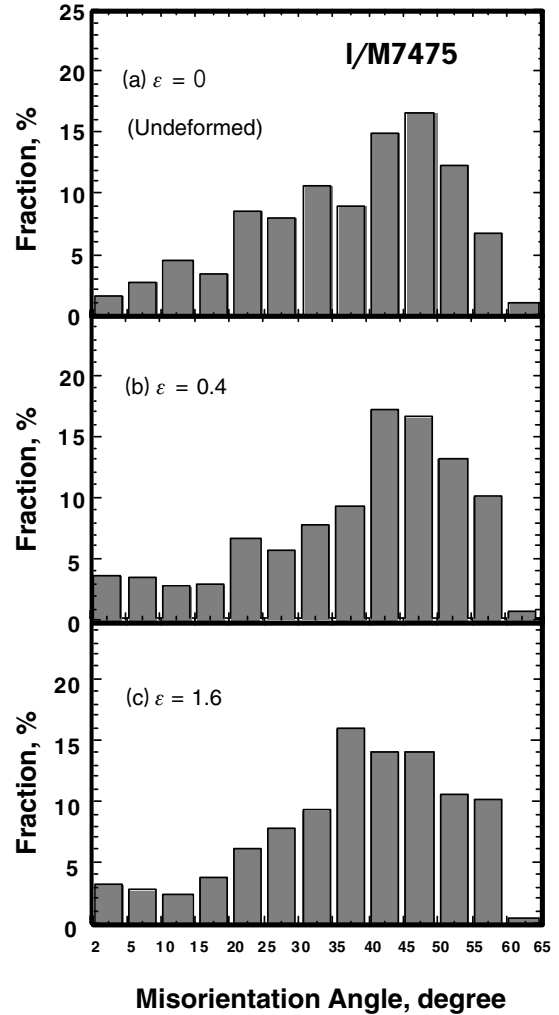


Figure 3 Distribution of misorientation angle at different strains for I/M7475 alloy.

3.1.2. Grain boundary structure in I/M7475

Histograms describing distributions of misorientation angles at the grain boundary before deformation and at 0.4 and 1.6 strains in I/M7475 is shown in Fig. 3a–c. During deformation, the distribution of misorientation angles at the grain boundary was almost unchanged, and the fraction of high-angle boundaries was high. The change in GBCD for I/M7475 are shown in Fig. 4.

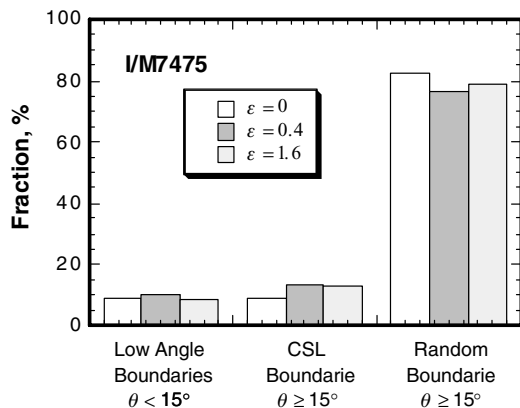


Figure 4 The variation in GBCD for I/M7475.

In I/M7475, the GBCD was defined by a high fraction of random boundaries and was almost unchanged during deformation. The fraction of coincident boundaries was almost unchanged with strain and was very low. It is well known that in superplastic deformation, the dominant deformation mechanism is GBS and the ratio of contribution of GBS to total elongation is 50–70% when tested under optimum conditions [29]. The GBS was influenced by the grain boundary structure, and GBS occurred easily at high angle and random boundaries [23, 24, 30]. It is therefore suggested that the contribution of GBS is high because the percentage of high angle and random boundaries is considerable during superplastic deformation.

3.2. Mechanical properties in P/M7475 compared with I/M7475

The stress-strain curves in P/M7475 and I/M7475 are shown in Fig. 5. Tensile tests were carried out at a temperature of 788 K in both materials. The strain rate in P/M7475 was 10^{-1} s^{-1} , and that in I/M7475 was $4 \times 10^{-5} \text{ s}^{-1}$. The elongation to failure in P/M7475 was almost the same with that in I/M7475, however, the stress-strain curve was different. In I/M7475, the gradual strain hardening due to grain growth occurred continuously up to failure. On the other hand, for P/M7475 after initial strain hardening, the flow stress reached an almost steady state, then decreased to failure. The variation in the m value with strain in both materials is shown in Fig. 6. In I/M7475, the m value was relatively

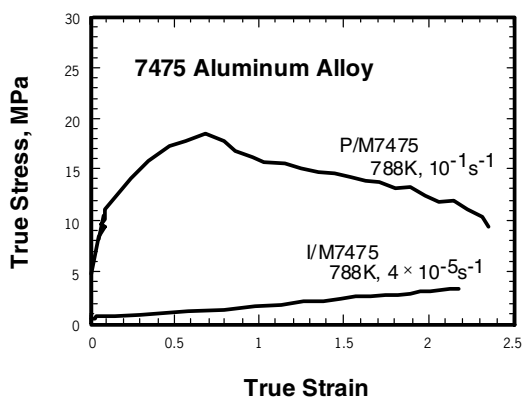


Figure 5 True stress—True strain curves for P/M and I/M 7475.

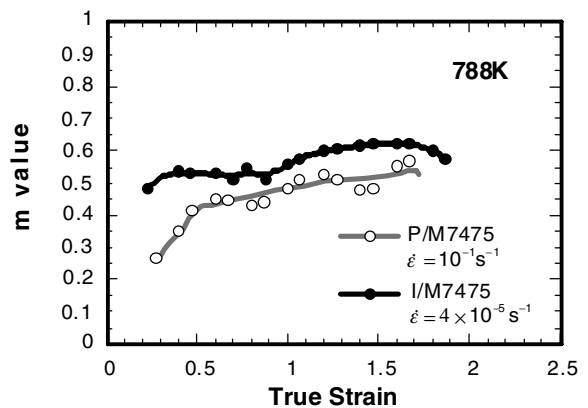


Figure 6 The variations in m value for 7475 aluminum alloys.

high (~ 0.5) and was almost constant during deformation. Conversely, in P/M7475, the m value was low at the initial stage of deformation; however, it increased as deformation proceeded. It is likely that the superplastic behavior in P/M7475 differs from that in conventional superplastic I/M7475 because of differences in the recrystallization process.

3.3. Deformation mechanism in P/M7475

GBS is a very important mechanism in superplastic deformation. Surface appearances of deformed specimens in P/M7475 are illustrated in Fig. 7. Observations at the grain boundaries with bright contrast attested to the occurrence of sliding along the grain boundaries, accompanied by the formation of striation bands. GBS occurred only partially at a strain of 0.4; more precisely, “cooperative grain boundary sliding” (CGBS) occurred. Zelin *et al.* [31] have reported that CGBS occurs in mechanically alloyed IN90211 alloy under high strain rates. CGBS means that a group of grains slides along the grain boundaries as a unit; in such cases, the apparent grain is thought to consist of a group of several subgrains. The apparent grain size was considerably larger than the actual grain size. It was therefore suggested that a group of grains deformed as a unit in P/M7475. The number of grains in the group decreased with increasing strain. Striation bands were stretched and showed winding with strain. Such features are associated with continuous GBS, as the grains rotate as deformation proceeds.

GBS was investigated quantitatively. The variation in the ratio of contribution of GBS to total elongation, r_{GBS} , with strain is shown in Fig. 8. In P/M7475, the r_{GBS} was low at an early stage of deformation. The r_{GBS} increased with the deformation progress and exhibited a high value of about 60%. This value is almost the same as the reported value of 50–70% in conventional superplastic materials [29]. It was therefore suggested that the dominant deformation mechanism changed from dislocation creep to GBS during deformation in P/M7475.

3.4. Microstructural evolution in P/M7475

A histogram describing distributions of misorientation angles at the grain boundary in P/M7475 before

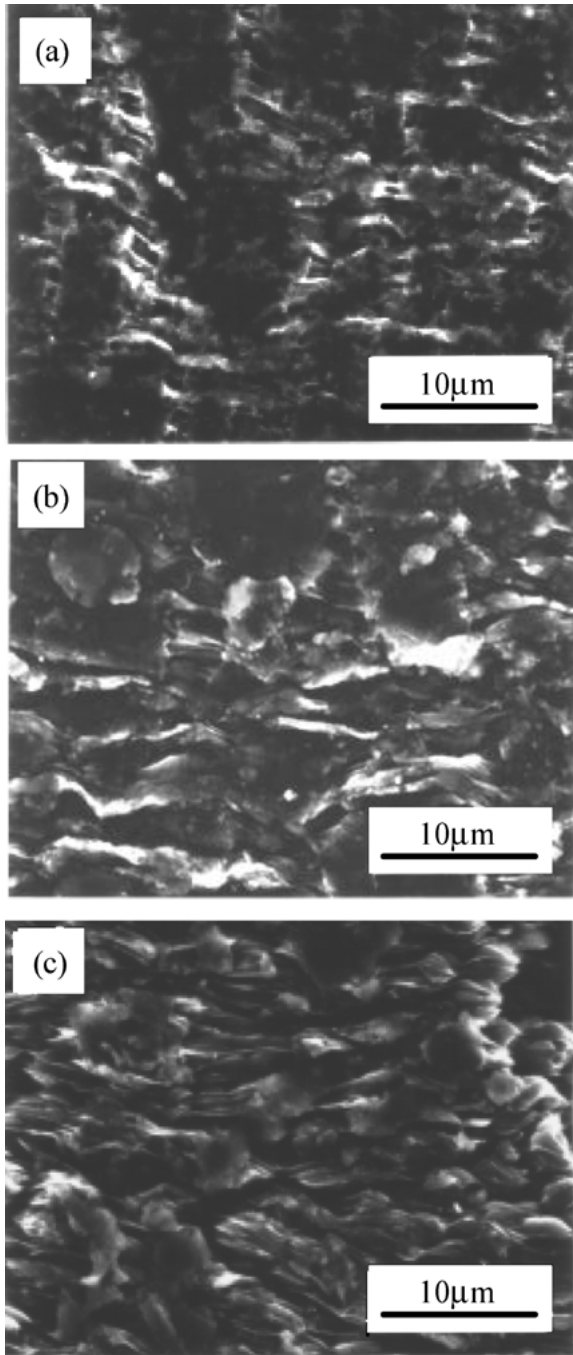


Figure 7 Surface appearances of P/M7475 alloy at: (a) 0.4, (b) 0.8, and (c) 1.6 strains.

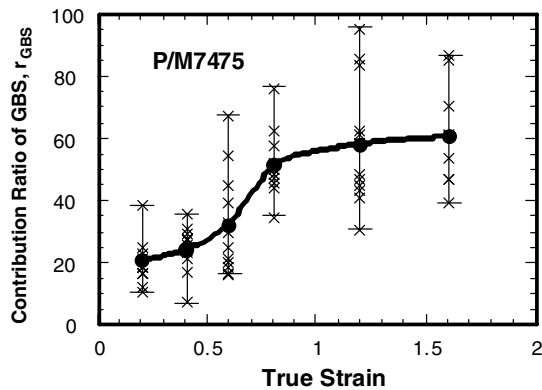


Figure 8 Variation of the contribution ratio of GBS to total elongation for P/M7475 alloy.

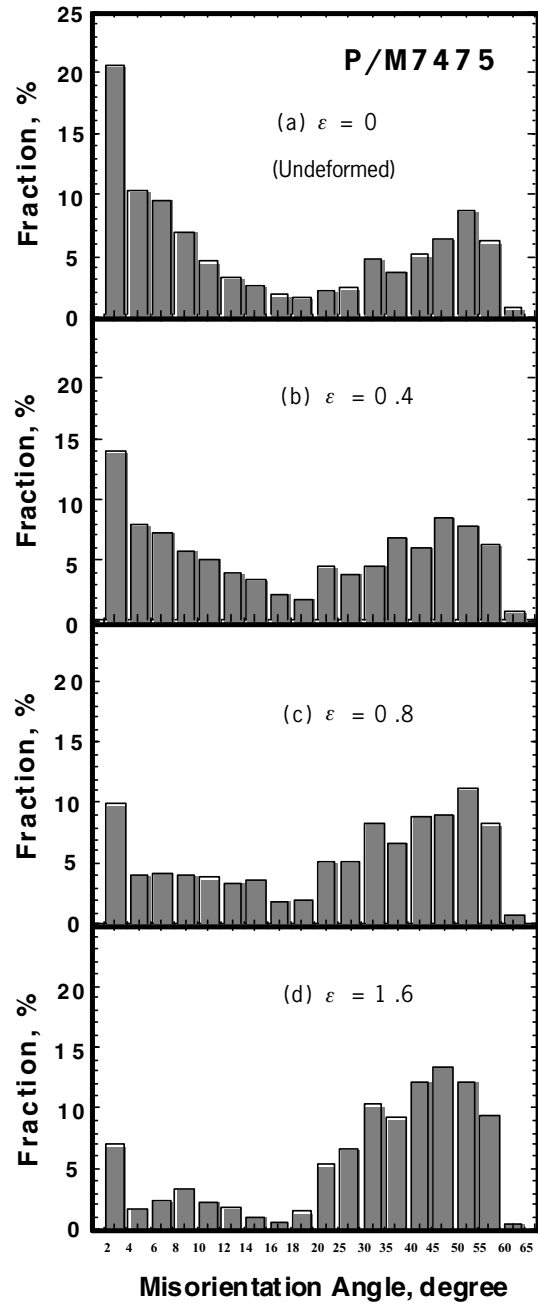


Figure 9 Distribution of misorientation angle at different strains for P/M7475 alloy.

deformation and at 0.4, 0.8 and 1.6 strains are shown in Fig. 9a–d. The microstructure in P/M7475 was not recrystallized structure and the fraction of low-angle boundaries was high before deformation. However, the misorientations at the grain boundary progressively evolved into higher angles with the deformation progress. In continuously recrystallized alloy, it has been reported that microstructure evolved during deformation [12, 32]. Matsuki *et al.* [12] have reported that the misorientations of sub-boundaries increased with increasing strain by CDRX in P/M7475-0.7Zr. Also McNelley *et al.* [32] have reported that in Al-10Mg-0.1Zr the frequency of high-angle boundaries increased by CDRX during deformation. The present result is similar to their results. Weinberg [30] has reported that grain boundary sliding was observed at boundaries having orientations $\geq 70^\circ$ under applied stress in aluminum.

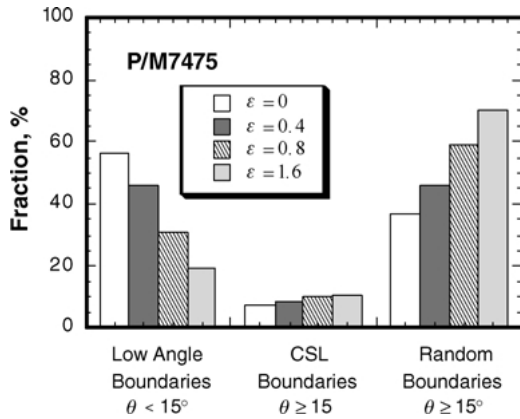


Figure 10 The variation in GBCD for P/M7475.

Therefore, the r_{GBS} increased during deformation because the fraction of boundaries having orientation $\geq 70^\circ$ increased with straining.

The change in GBCD for P/M7475 is shown in Fig. 10. The initial microstructure in P/M7475 was consisted of high fraction of low-angle boundaries. However, the percentage of random boundaries increased with the increment of straining. The fraction of coincident boundaries was almost unchanged with strain. Kokawa *et al.* [24] have reported that GBS occurred more easily at random boundaries than at coincident boundaries in aluminum because the grain boundary energy of random boundaries was higher than that of coincident boundaries. These results can be interpreted as evidence that the microstructure in P/M7475 is evolved by CDRX during superplastic deformation, and that the high r_{GBS} corresponds to the high fraction of high-angle and random boundaries as in conventional superplastic materials.

3.5. Accommodation process in P/M7475

GBS is the predominant deformation mechanism during superplastic flow, and GBS involves stress concentration at grain boundary triple junctions. It is necessary for cases of continuous GBS to accommodate the stress concentration. Therefore, the superplastic strain rate is limited by the accommodation process. It is recognized that stress concentration is accommodated by dislocation movements controlled by grain-boundary diffusion or lattice self-diffusion [22]. In order to determine the dominant diffusion process for superplastic flow in P/M7475, the activation energy was estimated by the temperature increment test. As shown in Fig. 8, the dominant deformation mechanism in P/M7475 at true strains of 0.8 and higher was GBS; the r_{GBS} was about 60%.

The activation energy for superplastic flow was estimated at a true strain of 1.2. We interrupted the tensile test at a true strain of 1.2 under the condition of a strain rate of 10^{-1} s^{-1} and 788 K, increased the temperature by 10 K quickly, and continued the tensile test at the same strain rate. The difference of true stresses at each temperature was examined; activation energy was measured from the constitutive Equation 1 ($n = 2$ in this equation). The activation energy for superplastic flow

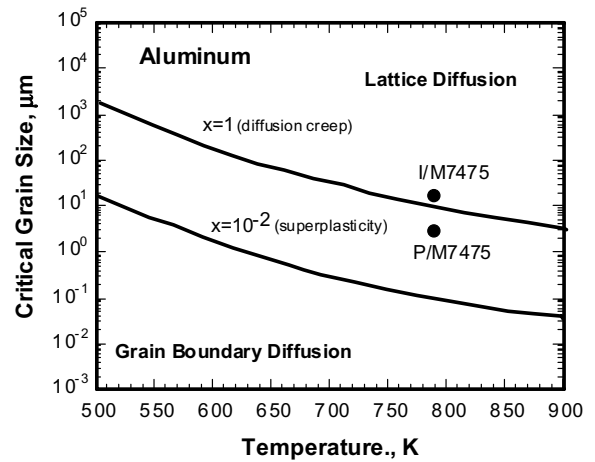


Figure 11 Variation in the critical grain size with temperature for aluminum based materials.

in P/M7475 was 138 kJ/mol, close to the reported value of the activation energy for lattice self-diffusion in Al (142 kJ/mol) [28]. Thus, the temperature increment test showed that the dominant diffusion process for superplastic flow in P/M7475 was lattice self-diffusion.

Also a dominant diffusion process for superplastic flow may be evaluated through the effective diffusion concept. The effective diffusion coefficient D_{eff} involving the lattice self-diffusion coefficient D_{L} and the grain-boundary diffusion coefficient D_{GB} is given by [33]

$$D_{\text{eff}} = D_{\text{L}} + x \frac{\pi \delta D_{\text{GB}}}{d}, \quad (3)$$

where x is an unknown constant and δ is the grain-boundary width. If the diffusion processes in superplastic flow are analogous with those in diffusion creep, x is unity. On the other hand, Metenier *et al.* [33] noted that $x = 10^{-2}$ for superplastic flow. The critical grain size above which a dominant diffusion process is lattice self-diffusion and below which it is grain-boundary diffusion can be evaluated by the effective diffusion concept. The critical grain size d_{C} is given by

$$d_{\text{C}} = \frac{x \pi \delta D_{\text{GB}}}{D_{\text{L}}}. \quad (4)$$

The variation in the critical grain size as a function of temperature is shown for aluminum-based materials in Fig. 11, where x is taken to be 10^{-2} and 1. The measured grain sizes for P/M and I/M7475 were lower than the critical grain size at $x = 10^{-2}$ at testing temperature. It is therefore suggested that the effective lattice self-diffusion is faster than the grain-boundary diffusion, so that a dominant diffusion process for superplastic flow in P/M7475 is lattice self-diffusion as well as that in I/M7475.

4. Discussion

The deformation mechanism during superplastic flow in P/M7475 is discussed. Data on flow stresses at fixed strains of 0.1, 0.8, 1.6 and 2.2 in P/M7475

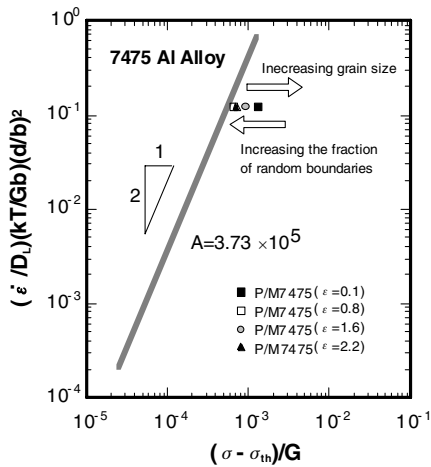


Figure 12 Relationship between $(\dot{\epsilon}/D_L)(kT/Gb)(d/b)^2$ and $(\sigma - \sigma_{th})/G$ for I/M7475.

are plotted in Fig. 12; those data were normalized for superplastic behavior. The relationship between $(\dot{\epsilon}/D_L)(kT/Gb)(d/b)^2$ and $(\sigma - \sigma_{th})/G$ for 7475 alloys is also shown in this figure. The data on flow stress at the fixed strain of 0.1 were in a good agreement with other data. However, the dominant deformation mechanism at an initial stage of deformation was not GBS, so that it was considered that the flow stress at a fixed strain of 0.1 was not flow stress for superplastic flow in P/M7475 and that the data at a strain of 0.1 was in a good agreement with the other data by accident. The flow stress at a strain of 0.8 was not in good agreement with the straight line with a slope of 2, even though the dominant deformation mechanism at a strain of 0.8 is GBS. On the other hand, it was clear that the flow stress at a strain of 2.2 in P/M7475 was close to a single straight line with a slope of 2. From the viewpoint of GBCD, it is suggested that the flow stress approaches a straight line with a slope of 2 as the percentage of random boundaries increased and was close to that in I/M7475.

The model of microstructural change in P/M7475 is considered. A schematic illustration of microstructural change in P/M7475 is shown in Fig. 13. The size of the apparent grain, consisting of almost-random boundaries, decreased with increases in the percentage of random boundaries. GBS occurs easily at random boundaries. The CGBS is attributed to the GBCD in P/M7475. In superplastic deformation, the flow stress decreases with decreasing grain size. It appears that the flow stress decreases due to decreases in the size of apparent grain that GBS occurs; i.e., increases in the fraction of random boundaries. It was also suggested that it is necessary to introduce a parameter for GBC into the constitutive equation for superplastic deformation in order to clarify the deformation mechanism in continuous dynamically recrystallized alloys. In this way, this figure shows that the data in the superplastic region of P/M7475 is in a good agreement with other investigation into I/M7475. It is therefore concluded that the dominant deformation mechanism for superplastic flow after CDRX in P/M7475 is GBS accommodated by dislocation movement controlled by lattice self-diffusion, similar to that in I/M7475.

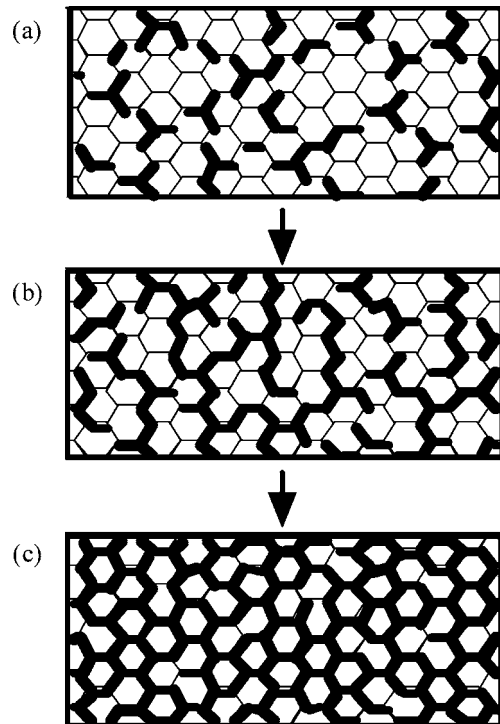


Figure 13 Schematic illustration of microstructural dynamics in P/M7475. The bold lines show random boundaries and the narrow lines show subboundaries. (a) Initial microstructure, (b) and (c) the microstructure during deformation.

5. Summary

1. P/M7475 was continuously and dynamically recrystallized. The microstructure in P/M7475 evolved into fine grains during deformation by CDRX. The fraction of high-angle and random boundaries increased with straining by CDRX. The deformation mechanism in P/M7475 was different from the conventional superplastic material due to this microstructural evolution.

2. At early stage of deformation, the dominant deformation mechanism in P/M7475 was dislocation creep. However, the contribution ratio of GBS to the total elongation increased as deformation progressed. The deformation behavior in P/M7475 changed from dislocation creep to superplasticity as the dominant deformation mechanism changed to GBS.

3. There was a close relationship between the grain boundary microstructure and GBS in P/M7475. A higher fraction of high-angle and random boundaries corresponded to a higher ratio of contribution of GBS to total elongation.

4. The activation energy for superplastic flow in P/M7475 was close to that for lattice self-diffusion in pure aluminum. Therefore, the dominant deformation mechanism during superplastic flow in P/M7475 was GBS accommodated by dislocation movement controlled by lattice self diffusion, as in I/M7475.

5. In P/M7475, CGBS was attributed to GBCD. The size of apparent grains in GBS was larger than that of subgrains. The apparent grain consisted of random boundaries and decreased with increasing fraction of random boundaries because GBS occurred easily at random boundaries. Therefore, the flow stress decreased with strain during superplastic flow in P/M7475.

References

1. H. IWASAKI, Y. IRIE, S. HAYAMI, K. HIGASHI and T. ITO, *J. Jpn. Inst. Light Met.* **39** (1989) 798.
2. M. K. RAO and A. K. MUKHERJEE, *Mater. Sci. Eng.* **80** (1986) 181.
3. D. H. SHIN, K.-T. PARK and E. J. LAVERNIA, *ibid.* **A 201** (1995) 118.
4. D. H. SHIN, C. S. LEE and W.-J. KIM, *Acta Mater.* **45** (1997) 5195.
5. J. XINGGANG, C. JIANZHONG and M. LONGXIANG, *Mater. Sci. Tech.* **9** (1993) 493.
6. Y. HIROSE, Y. MIYAGI, M. HINO and T. ETO, *J. Jpn. Inst. Light Met.* **36** (1986) 491.
7. Y. TAKAYAMA, T. TOZAWA and H. KATO, *Acta Mater.* **47** (1999) 1263.
8. K. HIGASHI, H. IMAMURA, T. ITO and S. TANIMURA, in "Superplasticity in Aerospace II," edited by T. R. McNelley and H. C. Heikkinen (The Minerals, Metals & Materials Society, 1990) p. 251.
9. T. HIRATA, T. MUKAI, N. SAITO, M. KOHZU, S. TANABE and K. HIGASHI, *Mater. Sci. Forum* **304-306** (1999) 333.
10. K. HIGASHI, S. TANIMURA and T. ITO, in Materials Research Society Symposium Proceedings, Vol. 196, edited by M. J. Mayo, M. Kobayashi and J. Wadsworth (1990) p. 385.
11. K. MATSUKI, G. STANIEK, H. NAKAGAWA and M. TOKIZAWA, *Z. Metallkde* **79** (1988) 231.
12. K. MATSUKI, T. IWAKI, M. TOKIZAWA and Y. MURAKAMI, *Mater. Sci. Tech.* **7** (1991) 513.
13. N. FURUSHIRO and S. HORI, in Materials Research Society Symposium Proceedings, Vol. 196, edited by M. J. Mayo, M. Kobayashi and J. Wadsworth (1990) p. 249.
14. W.-J. KIM, *Mater. Sci. Eng. A* **277** (2000) 134.
15. S. J. HALES and T. R. MCNELLEY, *Acta Metall.* **36** (1988) 1229.
16. T. R. MCNELLEY, E.-W. LEE and M. E. MILLS, *Metal. Trans.* **17A** (1986) 1035.
17. M. MABUCHI, J. KOIKE, H. IWASAKI, K. HIGASHI and T. G. LANGDON, *Mater. Sci. Forum* **170-172** (1994) 503.
18. B. M. WATTS, M. J. STOWELL, B. L. BAIKIE and D. D. E. OWEN, *Metal Sci.* **10** (1976) 189.
19. *Idem.*, *ibid.* **10** (1976) 198.
20. R. GRIMES, M. J. STOWELL and B. M. WATTS, *Metals Tech.* **3** (1976) 154.
21. T. G. LANGDON, *Metall. Trans. A* **13A** (1982) 689.
22. O. D. SHERBY and J. WADSWORTH, in "Deformation Processing and Microstructure," edited by G. Krauss (ASM, Materials Park, OH, 1984) p. 355.
23. T. WATANABE, *Mater. Sci. Eng. A* **166** (1993) 11.
24. H. KOKAWA, T. WATANABE and S. KARASHIMA, *Phil. Mag. A* **44** (1981) 1239.
25. S. I. WRIGHT, *J. Comp. Ass. Microscopy* **5** (1993) 207.
26. F. A. MOHAMED, *J. Mater. Sci.* **18** (1983) 582.
27. R. S. MISHRA, T. R. BIELER and A. K. MUKHERJEE, *Acta Metall. Mater.* **43** (1995) 877.
28. H. J. FROST and M. F. ASHBY, in "Deformation-Mechanisms Maps" (Pergamon Press, 1982) p. 21.
29. Z. R. LIN, A. H. CHOKSHI and T. G. LANGDON, *J. Mater. Sci.* **23** (1988) 2712.
30. F. WEINBERG, *Tras. Metal. Soc. AIME* **212** (1958) 808.
31. M. G. ZELIN, T. R. BIELER and A. K. MUKHERJEE, *Metal. Trans.* **24A** (1993) 1208.
32. T. R. MCNELLEY, M. E. MCMAHON and S. J. HALES, *Scr. Mater.* **36** (1997) 369.
33. P. METENIER, G. G. DONCEL, O. A. RUANO, J. WOLFENSTINE and O. D. SHERBY, *Mater. Sci. Eng. A* **215** (1990) 195.

*Received 7 January
and accepted 19 June 2003*